

Polyurethane Vitrimers Engineered with Nitrogen-Coordinating Cyclic Boronic Diester Bonds for Sustainable Bioelectronics

*Yue Tao, Yu Xue, Fucheng Wang, Liangjie Shan, Zhipeng Ni, Yunting Lan, Pei Zhang, Yafei Wang, and Ji Liu**

Flexible bioelectronic devices seamlessly interface with organs and tissues, offering unprecedented opportunity for timely prevention, early diagnosis, and medical therapies. However, the majority of flexible substrates utilized in bioelectronics still encounter significant challenges in terms of recyclability and reprocessing, leading to the accumulation of environmentally and biologically hazardous toxic waste. Here, the study reports the design of recyclable polyurethane (PU) vitrimers engineered with internal boron-nitrogen coordination bonds that can reversibly dissociate to boronic acids and hydroxyl, or undergo metathesis reaction following an associative pathway. The study demonstrates the capacity of these recyclable PU vitrimers as flexible substrates in various wearable and implantable bioelectronic applications, achieving high-quality electrophysiological recordings and stimulation. Furthermore, the study establishes a sustainable recycling process by reconstructing a range of bioelectronic devices from the recycled PU vitrimers without compromising the mechanical performance. This closed-loop approach not only addresses the critical challenge of the reclaiming medical electronic waste but also paves the way for the development of sustainable flexible bioelectronics for healthcare applications.

precise, real-time physiological monitoring and therapeutic interventions.^[1–5] With the rapid advancements in soft material synthesis and cutting-edge micro/nanofabrication technologies, a wide array of epidermal sensors, electronic skins/tattoos, and implantable bioelectronics has been developed.^[2,4,6,7] These advancements have significantly improved the compatibility and functionality of these devices, paving ways for transformative healthcare applications and personalized medicine.^[1,7,8] However, the mass production and relatively short lifespan of flexible bioelectronics have inevitably resulted in a significant volume of medical electronic waste (e-waste), culminating in significant resource wastage, environmental contamination, and potential human health risks.^[9–11] Therefore, there is an urgent need for recyclable flexible bioelectronics to reduce resource wastage and to mitigate adverse environmental and health impacts associated with biomedical e-waste.^[12–14]

1. Introduction

Flexible bioelectronic devices seamlessly integrate with the living body, revolutionizing biomedical sciences by enabling

Structurally, flexible bioelectronics are typically constructed from polymer-based and hybrid electronic materials.^[1,13,15,16] Polymers are predominantly utilized as substrates and encapsulation layers, providing structural integrity and sealing functions for flexible electronics. Although existing flexible bioelectronics have primarily been fabricated using silicone elastomers, their stable chemical cross-linking prevents them from being recycled and reprocessed, presenting challenges for the recycling of flexible bioelectronics.^[11,17,18] Recently, polymers functionalized with dynamic bonds have attracted significant interest, as they offer a promising solution to the recycling and reprocessing challenges associated with traditional thermoset plastics.^[11,19] Polymers composed of dynamic noncovalent bonds, in particular, exhibit rapid and sensitive reconstructive capacities, facilitating straightforward recycling and reprocessing, and have been extensively explored in recyclable flexible bioelectronics.^[20,21] Nonetheless, these materials are generally susceptible to environmental factors such as temperature and humidity, and exhibit unsatisfactory mechanical performance and stability owing to the relatively weak cross-linking, which is unfavorable for durable applications in complex environments.^[20,22] Covalent adaptable networks (CANs) represent a category of crosslinked polymer

Y. Tao, Y. Xue, F. Wang, L. Shan, Z. Ni, Y. Lan, P. Zhang, Y. Wang, J. Liu
 Department of Mechanical and Energy Engineering
 Southern University of Science and Technology
 Shenzhen 518055, P. R. China
 E-mail: liuj9@sustech.edu.cn

Y. Xue
 Jiangxi Province Key Laboratory of Flexible Electronics
 Flexible Electronics Innovation Institute
 Jiangxi Science and Technology Normal University
 Nanchang, Jiangxi 330013, P. R. China

J. Liu
 Shenzhen Key Laboratory of Biomimetic Robotics and Intelligent Systems
 Department of Mechanical and Energy Engineering
 Southern University of Science and Technology
 Shenzhen 518055, P. R. China

 The ORCID identification number(s) for the author(s) of this article can be found under <https://doi.org/10.1002/smll.202408557>

DOI: 10.1002/smll.202408557

systems characterized by the presence of dynamic covalent bonds, integrating the advantages of dynamic bonds with thermosetting polymers, thereby endowed with self-healability, degradability, recyclability, as well as exceptional mechanical performance and durability.^[23–30] Particularly, associative CANs, also known as the vitrimers, can be reprocessed in a manner akin to malleable silica materials, offering a promising pathway for the development of sustainable bioelectronics.^[30–34] Although significant strides have been made in the developing vitrimers with various dynamic covalent bonds, such as ester bond, urea bond, carbamate bond, imine bond, disulfide bond, and boronic ester bond, increasing the robustness of the dynamic bonds and stability of vitrimers while maintaining relatively mild recycling conditions remains a challenge.^[30,35,36] Specifically, boronic ester bonds are susceptible to hydrolysis;^[37] the exchange reactions of ester and carbamate bonds often necessitate catalysts, which can leach out and may result in catalyst deactivation and potentially introduce health risks.^[38,39] Furthermore, some other harsh reaction conditions are often necessary for the exchange reactions to occur, such as elevated temperatures, acidic conditions, or other chemical agents.^[30,40–42] These challenges could lead to deteriorated performance of both original and recycled materials, as well as potential health risks when used in bioelectronics.^[16,40,43–47] Therefore, they are still rarely explored in fabricating flexible bioelectronics. To address these potential issues, it is imperative to develop vitrimer materials, which not only exhibit superior environmental stability but also is capable of high-quality recovery via a non-destructive and environment-friendly recycling process.

In this study, we developed a recyclable polyurethane (PU) vitrimers suitable for use as a flexible substrate/encapsulant for various bioelectronics, enabling high-fidelity interfacing with biological tissues, and offering the capability for recycling and reusing (Figure 1a,b). This unique dynamic cross-linked network allowed PU recyclable in both solid and liquid phases and maintain reliable characteristics after recycling, thus controllable recycling and reprocessing of the bioelectronics. Furthermore, the soft and biocompatible characteristics of NCB-PU-based bioelectronics allowed them as wearable stimulators for precisely modulating electrical activity in peripheral nerves of the hands, as well as implantable epicardial bioelectronic patches for the monitoring and treatment of cardiac diseases. These results demonstrated that the design and fabrication of sustainable bioelectronics provide a groundbreaking platform for advancing the next-generation biointerfacing technologies.

2. Results and Discussion

2.1. Design and Synthesis of NCB-PU Vitrimers

To validate our design rationale, we selected polyurethanes (PUs) as the polymer backbone due to their intriguing attributes such as mechanical flexibility, stretchability, and ease of chemical modification.^[48] To endow PU with recyclability, we employed internal nitrogen-coordinated boronic esters as linkages to construct the dynamic covalent network within PU. Boronic ester bonds are characterized by their high bond energy and have been widely applied in the creation of recyclable vitrimers, owing to their dynamic nature. The bond exchange reactions occur spontaneously without the addition of catalysts or chemicals at low

temperatures, thereby facilitating a facile and environmentally benign recycling process.^[49] In particular, cyclic boronic esters with internal boron-nitrogen coordination in these systems have been investigated to overcome the issue of hydrolytic instability associated with conventional boronic ester bonds in commonly used environments.^[42] While the internal boron-nitrogen coordination bond will be dissociated upon heating, leading to the transformation of the five-membered ring into eight-membered ring and the increase of ring strain, which result in a decrease in thermal and hydrolytic stability and an increase in the bond dynamicity.^[50] Therefore, hydrolysis can still be induced by specific external stimuli, such as elevated temperatures and chemical agents.^[42,50] The nitrogen-coordinating cyclic boronic diester (NCB) compound as a diol monomer was first synthesized through the condensation between 4-(hydroxymethyl) phenylboronic acid and triethanolamine, and its chemical structure was confirmed by ¹H NMR spectroscopy (Scheme S1 and Figure S1, Supporting Information). NCB-based polyurethane (NCB-PU) was prepared through a one-pot multi-step polyaddition reaction process using carbamate chemistry in the presence of catalyst dibutyltin dilaurate (DBTDL) (Scheme S2, Supporting Information). Initially, the isocyanate-terminated polyurethane prepolymer was synthesized by reacting isophorone diisocyanate (IPDI) with polyethylene glycol (HO-PEG-OH). This was followed by the sequential addition of NCBC and the remaining IPDI, subsequently, the crosslinking agent trimethylolpropane (TMP) was added for the final polymerization step. The structure of NCB-PU was characterized via Fourier transform infrared (FTIR) spectroscopy. As shown in Figure S2 (Supporting Information), the characteristic peaks at 3325 and 1710 cm⁻¹ corresponded to the N-H and C=O bonds from PU, respectively. The disappearance of the peak between 2200–2280 cm⁻¹ indicated the complete conversion of isocyanate moieties. Incorporation of boronic ester moieties into the NCB-PU was confirmed by the B-O characteristic peak at \approx 1353 cm⁻¹. These results confirmed the successful synthesis of NCB-PU vitrimers. As illustrated in Figure 1c,d, the incorporation of NCB into the polymer matrix forms a dynamic crosslinked network, conferring the PU vitrimers with exceptional recyclability. When subjected to heating, the bond exchange reactions within the PU vitrimer facilitate efficient stress relaxation, thereby granting superior reprocessability. Additionally, a notable feature of the PU vitrimers is its capacity to undergo hydrolysis when exposed to an excess of water, leading to the depolymerization into oligomers. Subsequent removal of water triggers re-esterification reactions, thereby reconstituting the cross-linked network. This reversible behavior underscores the potential application of NCB-PU vitrimers for sustainable bioelectronics.

2.2. Key Properties of NCB-PU Vitrimers

Superior chemical and thermal stability are crucial for the reliability and longevity of flexible bioelectronic devices. The NCB-PU vitrimers samples exhibited remarkable stability against various solvents, for example, DMF, due to their covalently cross-linked structure. During a 2-h exposure in DMF at high temperature (130 °C), the NCB-PU samples retained swollen rather than completely dissolved (Figure S3, Supporting Information), signifying

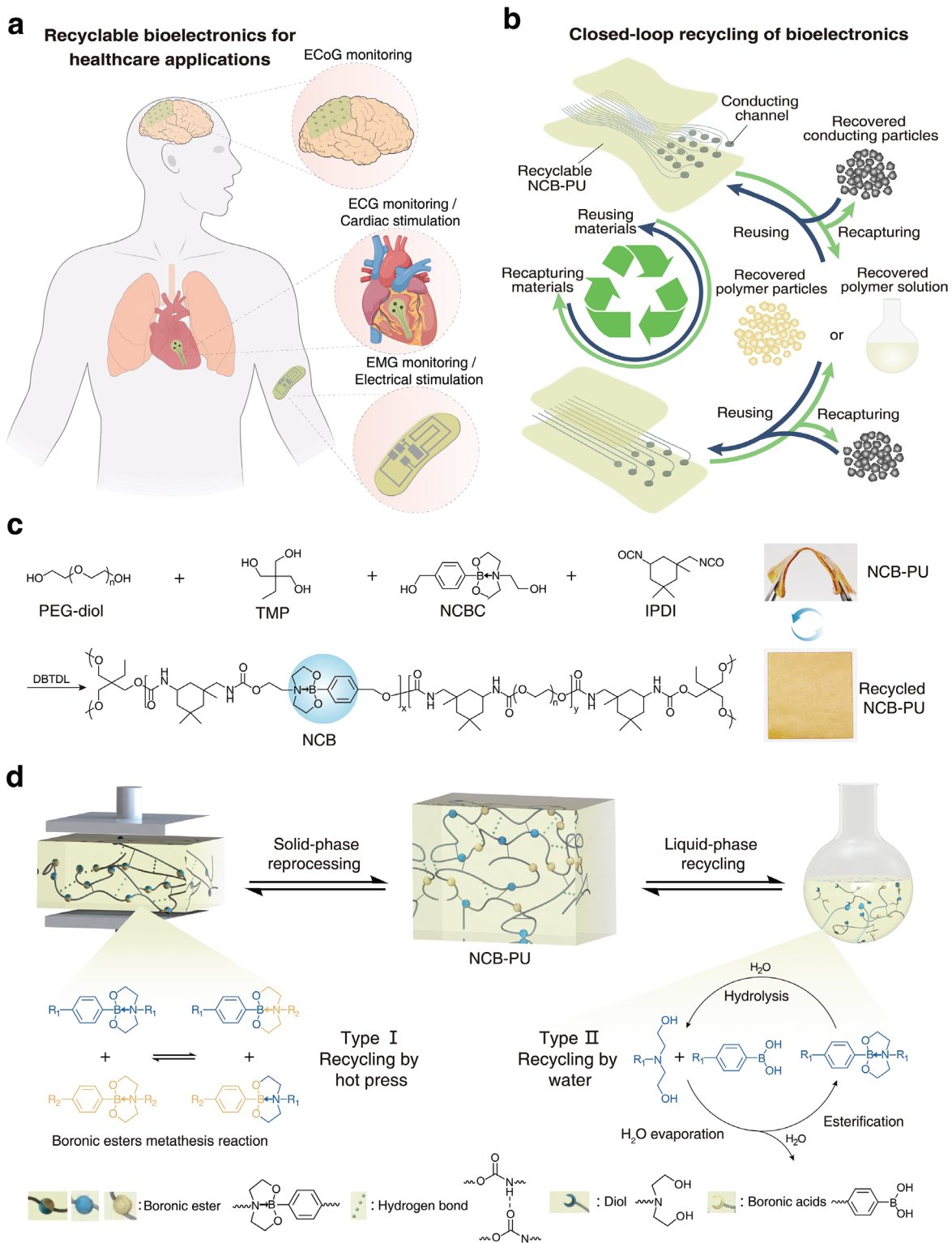


Figure 1. Recyclable polyurethane vitrimers for sustainable bioelectronics. a) Schematic illustration of recyclable bioelectronics for various physiological signals monitoring, including electroencephalogram (EEG), electrocardiograms (ECG), and electromyogram (EMG). b) Recycling process of NCB-PU-based bioelectronics. The NCB-PU-based bioelectronics can be recycled in either the liquid or solid phase, and the recycled materials can be further reprocessed into wearable/implantable electronics with customized structures. c) Chemical structure of the NCB-PU vitrimers synthesized from PEG-diol, TMP, NCBC, and IPDI. The NCB-PU vitrimer samples exhibited superior flexibility under mechanical bending. d) Schematic diagram of the proposed mechanism for recyclable NCB-PU vitrimers and reversible reaction of NCB linkages in PU networks induced by water or boronic esters metathesis reaction.

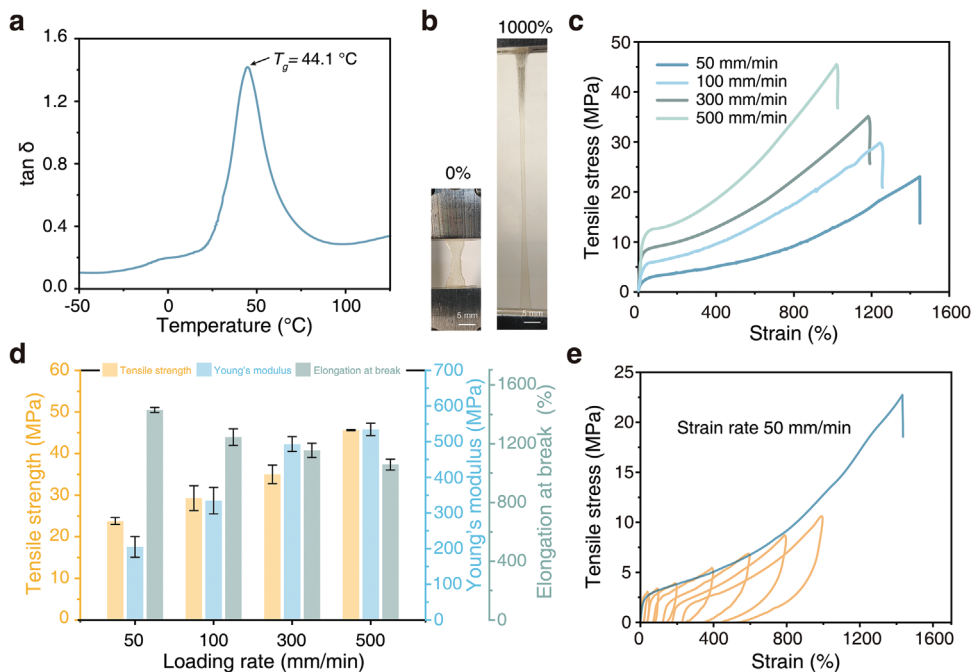


Figure 2. Properties of the NCB-PU vitrimers. a) $\tan \delta$ curves of the NCB-PU vitrimers. b) Digital photographs of the NCB-PU vitrimers samples before and upon stretching. Scale bar: 5 mm. c) Representative stress-strain curves of the NCB-PU vitrimer samples at different deformation rates (50–500 mm/min). d) Summary of tensile strength, Young's modulus, and elongation at break for NCB-PU vitrimers samples at different deformation rates. e) Representative stress–strain hysteresis curves obtained from cyclic tests of NCB-PU vitrimers at different strain ranges (50%, 100%, 200%, 400%, 600%, 1000% strain). Data in (d) are presented as means \pm standard deviation (S.D.), $n = 5$.

the maintenance of the structural integrity, which could ensure the consistent performance of flexible bioelectronics across some harsh environmental conditions. Thermal properties of NCB-PU were studied with dynamic mechanical analyses (DMA) and thermogravimetric analysis (TGA). The DMA profiles of NCB-PU showed that the glass transition temperature (T_g) was $\approx 44\text{ }^{\circ}\text{C}$ (Figure 2a). The TGA results demonstrated the superior thermal stability with a weight loss below 5% at $248\text{ }^{\circ}\text{C}$ (Figure S4, Supporting Information), meeting the thermal processing requirements for the polymer substrate.

The mechanical performance of the NCB-PU vitrimers is comprehensively studied with a tensile machine. The NCB-PU vitrimers generally exhibit superior stretchability, capable of withstanding strains exceeding 1000% without fracturing (Figure 2b). We further conduct tensile tests to quantify the mechanical performances of the NCB-PU vitrimers at different deformation rates. As shown in Figure 2c,d, the NCB-PU film exhibited excellent stretchability with a strain of over 1400% at a deformation rate of 50 mm min^{-1} . Even at a high loading rate of 500 mm min^{-1} , the NCB-PU film exhibited a stretchability up to ten times its original length, indicating robust deformation capacity even under rapid deformation. This remarkable deformation capacity is hypothesized to arise from the dynamic nature of the hydrogen bonding and the reversible B-N coordination bonds in the cyclic boronic esters.^[51] The hydrogen bonding in NCB-PU rapidly fractures and reforms upon stress loading, while the reversible B-N coordination facilitates the transition between five- and eight-membered boronic esters during the tension.^[51,52] Furthermore, the stable dynamic covalent B-O bonds contribute to maintaining the network's structural integrity and cross-linking density.

During sequential cyclic tensile testing (50%, 100%, 200%, 400%, 600%, 1000% strain) without rest between two cycles, NCB-PU exhibited appreciable residual strain due to the reformation of dynamic noncovalent bonds at new sites, facilitating energy dissipation (Figure 2e). Moreover, the tensile stresses remained largely unaffected across cycles, indicating the preservation of the covalent network's integrity.^[53,54] Consequently, the NCB-PU film exhibits high stretchability and favorable toughness, making it a promising material candidate for applications involving movement and deformation, such as interfacing with a periodically beating heart.

2.3. Recyclability of the NCB-PU Vitrimers

The high bond energy of the B-O bond confers NCB-PU vitrimers with robust mechanical properties, yet it also permits a reversible metathesis reaction via an associative exchange mechanism, thus endowing the materials with vitrimers characteristics, such as reprocessability.^[49] Upon subjecting to thermal treatment, the dissociation of B-N coordination bonds and hydrogen bonds facilitates the dynamic exchange of boronic ester linkages. As demonstrated in Figure 3a, small pieces of NCB-PU samples can be reprocessed via compression molding at $130\text{ }^{\circ}\text{C}$ and 2 MPa pressure for 15 minutes. It is deserved to mention that the NCB-PU samples could be readily reprocessed over three cycles without tuning the processing parameters, corroborating the intriguing recyclability. The recycled films maintained the same chemical stability as the original one. The FTIR spectroscopy and TGA curve revealed no substantial change compared to those of

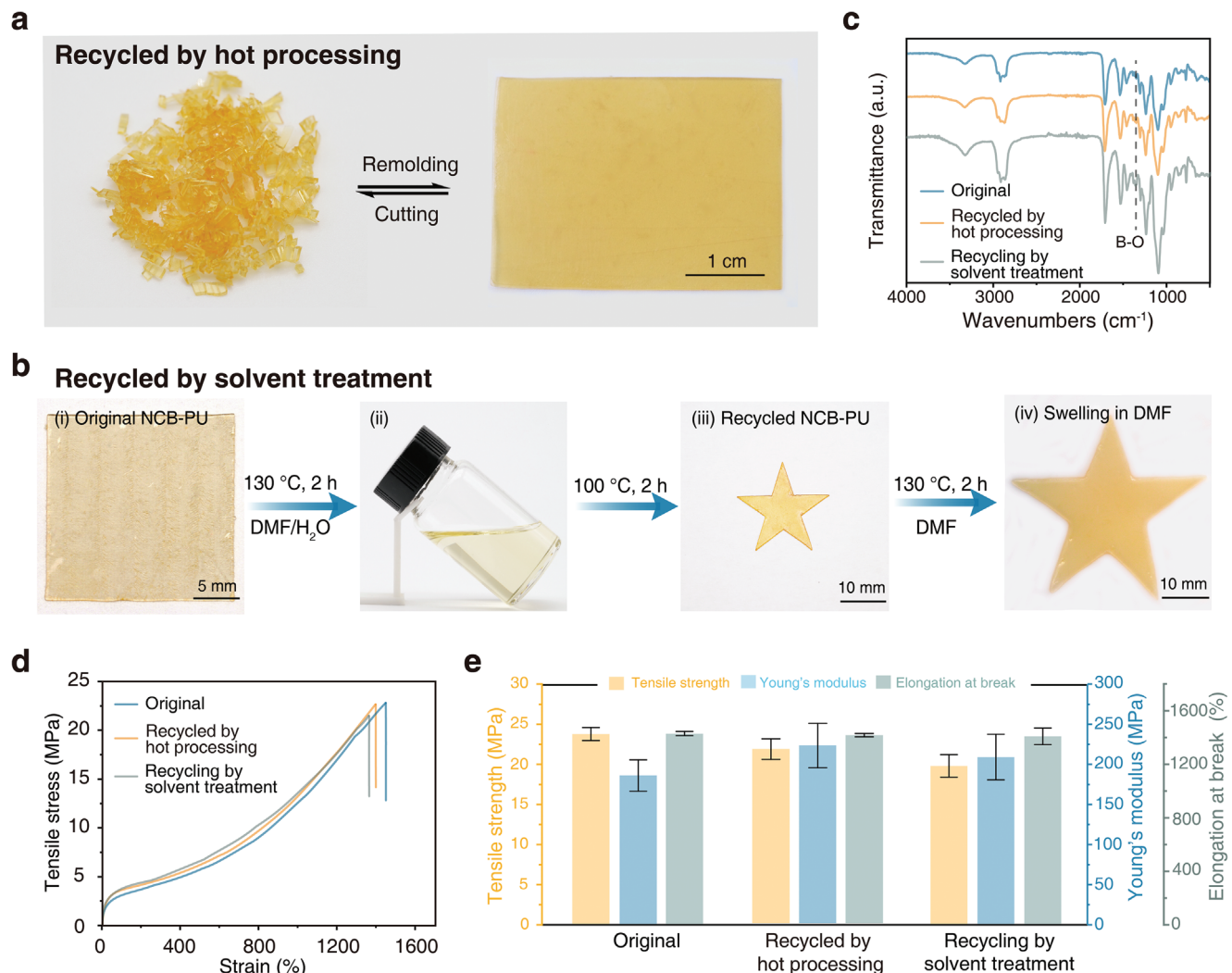


Figure 3. Recyclability of NCB-PU vitrimers. a) Images recording the reprocessing of NCB-PU vitrimers from fractured pieces into a new film through thermal processing. Scale bar: 1 cm. b) Images recording the reprocessing of NCB-PU vitrimers (i) by completely dissolving within DMF/H₂O mixture (ii), and reconstruction upon removing DMF/H₂O at 100 °C for 2 h (iii). The recycled NCB-PU sample was swollen, other than completely dissolved, in DMF at 130 °C for 2 h in the absence of H₂O (iv). c) Representative FT-IR spectra, d) stress–strain curves, and e) summary of mechanical attributes of the recycled NCB-PU vitrimers by hot processing and solvent treatment. The data in e are presented as the mean \pm S.D., $n = 5$.

the original NCB-PU samples, corroborating the preservation of the chemical composition and structure upon thermal recycling (Figure 3c; Figures S4 and S5, Supporting Information). Additionally, Figure 3d and Figure S6 (Supporting Information), illustrated that the stress–strain curves of the recycled NCB-PU nearly coincide with those of the initial NCB-PU, and Figure 3e showed that there was no evident decrease in tensile strength, Young's modulus, or elongation at break even after three-cycle reprocessing. Furthermore, the glass transition temperature (T_g) as determined by DMA showed no appreciable alteration over the three reprocessing cycles (Figure S7, Supporting Information). These results confirmed the exceptional recyclability of the NCB-PU vitrimers through a thermal process, in the absence of catalysts or solvents.

In addition to metathesis reaction, boronic esters also subject to hydrolysis/re-esterification through a dissociative exchange mechanism, facilitating the effective liquid-phase recycling of

NCB-PU vitrimers. Although boronic esters with B-N internal coordination exhibit improved hydrolytic stability under ambient conditions, hydrolysis can still be induced by specific external stimuli, such as elevated temperatures and chemical agents.^[55,56] We further investigated the water-induced degradation and recycling of NCB-PU vitrimers according to the process of Scheme S3 (Supporting Information), using a water-DMF mixed solvent as the recycling medium. DMF was chosen for its solubility with water and its ability to swell the NCB-PU vitrimers, allowing water molecules to interact with boronic ester groups and trigger the hydrolysis. The NCB-PU vitrimer samples were soaked in a mixed solvent of DMF and water with a volume ratio of 4:1 and subjected to vigorous stirring and incubation at 130 °C. The NCB-PU vitrimers gradually disintegrated and eventually completely dissolved, due to the destruction of the chemical equilibrium of the cross-linked network by the hydrolysis reactions in the presence of water molecules. Dynamic light scattering (DLS)

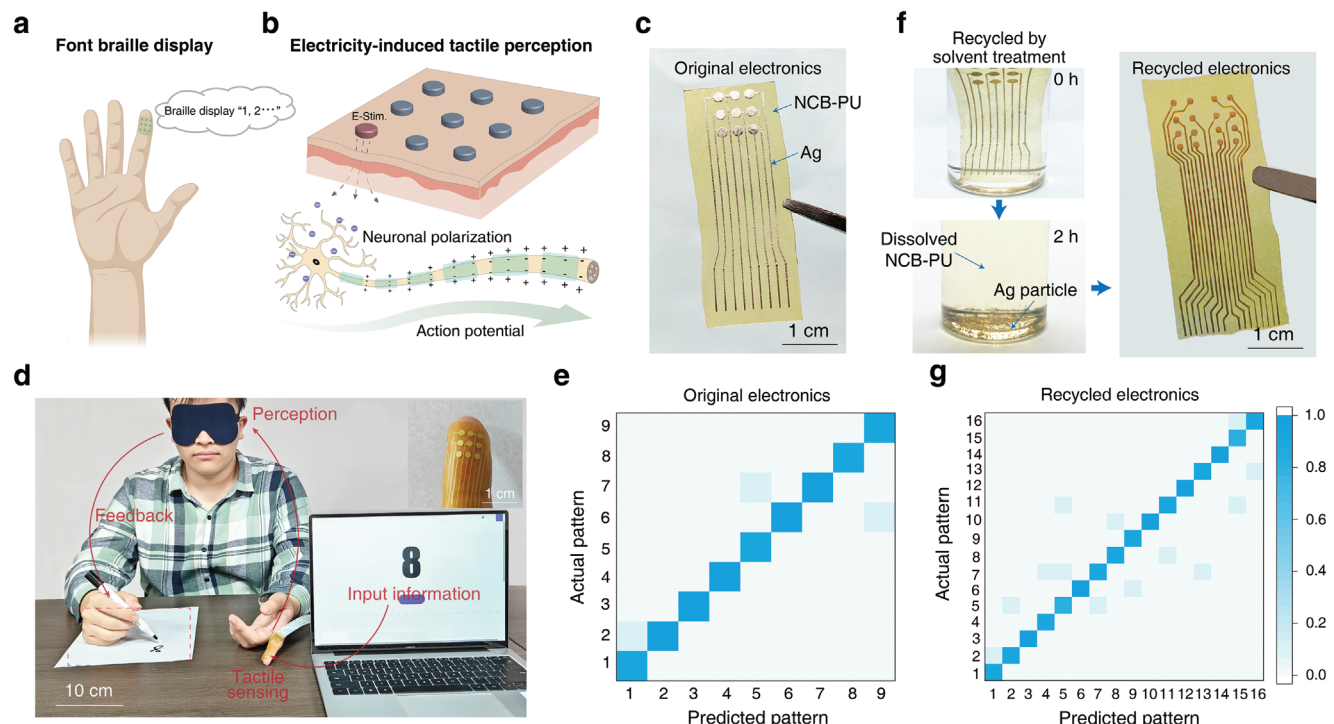


Figure 4. NCB-PU vitrimers as a flexible substance for sustainable wearable electronics. **a)** Schematic of digital information transmission through the wearable electronics. **b)** Schematic illustration the mechanism of tactile perception. The induction of current within the skin serves to activate mechanoreceptors and nerves, resulting in the generation of action potentials that are subsequently decoded by the brain as tactile information. **c)** Image of the wearable electronics equipped with nine autonomous channels. Scale bar: 10 mm. **d)** Demonstration of precise positioning of the stimulus site by wearable electronics. Insert is the image of the recycled electronics with nine independent channels. **f)** Image of the solvent-induced recovery of NCB-PU-based bioelectronics. **e–g)** Confusion map of the positioning results as measured by using the original **e)** and recycled **g)** electrodes.

analysis revealed that the particle size of the oligomers resulting from the degradation process falls within the range of 1–100 nm (Figure S8, Supporting Information). After the removal of DMF and water, the oligomers can be re-esterified to reform the NCB-PU vitrimers. Moreover, the recycled NCB-PU vitrimers exhibited structural swelling, other than completely dissolved, during a 2-h incubation in DMF at 130 °C, suggesting the reinstatement of the cross-linked network (Figure 3b).

The FTIR spectrum and TGA curve were essentially identical to those of the original NCB-PU vitrimer samples, corroborating the complete restoration of NCB-PU vitrimers after hydrolysis/re-esterification recycling process (Figure 3c; Figure S4, Supporting Information). The mechanical properties of the recycled NCB-PU vitrimers were similar to those of the original NCB-PU vitrimers (Figure 3d,e). These results demonstrate that the NCB-PU vitrimers can be easily recycled under relatively mild conditions without the need for any catalysts. This is of great significance for enabling the complete recovery of matrix resin and expensive fillers from composite materials, while preserving their performance.^[45,46,57]

2.4. NCB-PU-Based Bioelectronics for Electrical Modulation of Peripheral Neural Systems

Figure 4a introduces an array of wearable electrode, ingeniously designed for integration with human skin, in order to deliver

tactile stimulation through electrical modulation. Wearable electronics generate electric stimulus at targeted regions of the skin, leading to the initiation of action potentials along the axons of adjacent mechanoreceptors. These action potentials travel in an upstream direction via identical neural conduits and are decoded by the brain as tactile perceptions (Figure 4b).^[58,59] Utilizing NCB-PU vitrimers as a flexible substrate, we fabricated a 3 × 3 array of silver electrodes using direct ink writing-based 3D printing technology.^[60,61] The resulting electrodes are both flexible and stretchable, ensuring a comfortable interface on the biological tissues (Figure S9, Supporting Information). This conformal attachment guarantees optimal interface between the electronic components and the skin's irregular surface, thereby guaranteeing the precise positioning of the stimulus site. Thanks to the improved interface contact, a stimulation voltage ranging from 10 to 20 V is adequate to evoke a spectrum of tactile perceptions, encompassing subtle tactile sensations to more pronounced sharp prickly feelings. Additionally, we developed a closed-loop feedback system that includes a wearable electrode array for skin contact, an electric stimulator for voltage output, a control system for regulating the stimulus pathway, and a display device for data input (Figure 4d; Movie S1, Supporting Information). To assess the precision of tactile perception, we arranged the nine stimulation sites to correspond to the numbers 1 through 9, and administered random electrical stimulations to volunteers. As illustrated in Figure 4e, tests conducted with volunteers yielded a recognition accuracy exceeding 90%, demonstrating the seamless

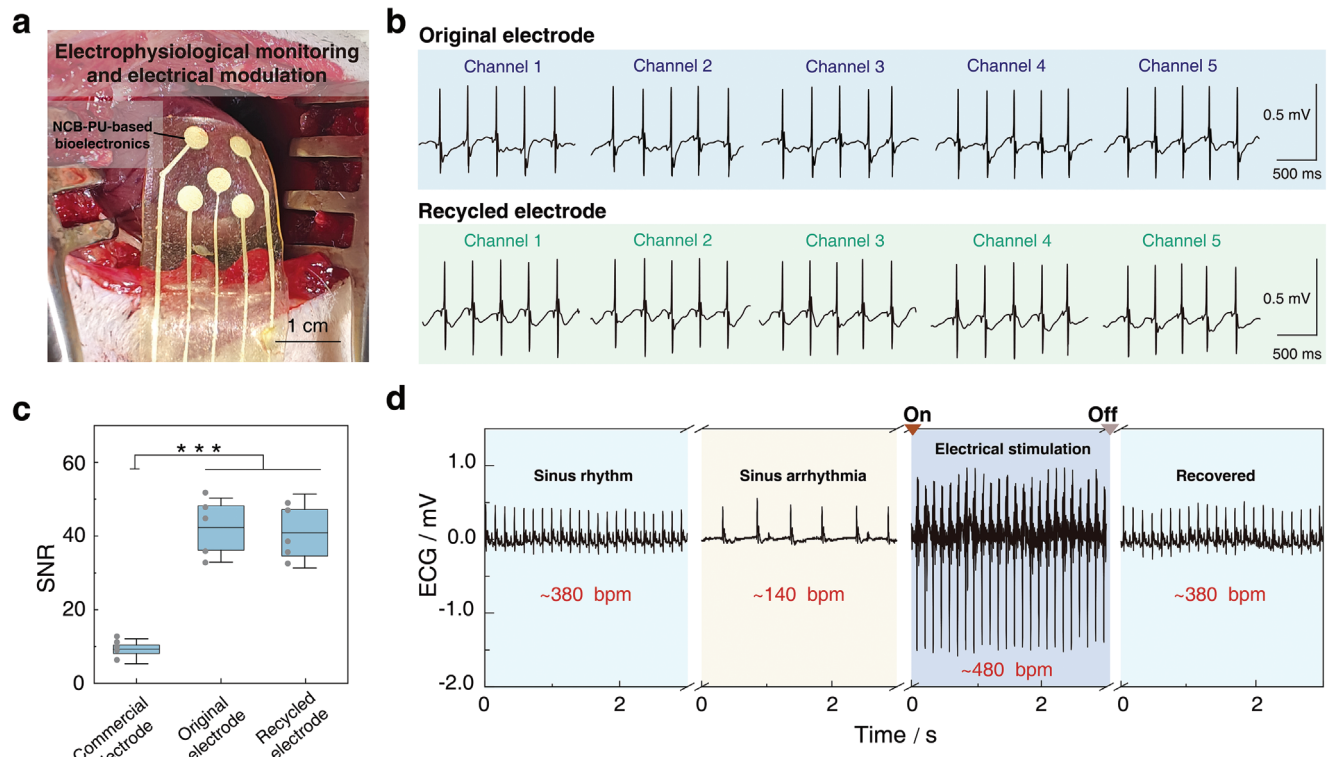


Figure 5. In vivo epicardial recording and electrical pacing in a rat model with the NCB-PU-based bioelectronics. a) Image of an open-chest procedure with the NCB-PU-based bioelectronics conformally attached onto the ventricular epicardium for epicardial recording and electrical pacing. Scale bar: 1 cm. b) 5-channel ECG signals from the rat heart recorded with the NCB-PU-based bioelectronics. Similar epicardial ECG traces were acquired for the original (top) and recycled (bottom) electrodes. c) Distinct difference in signal-to-noise ratio (SNR) is detected from the commercial metallic needle electrode, original and recycled NCB-PU-based electrodes. The data in c are presented as the mean \pm S.D., $n = 5$. d) Demonstration of cardiac electrical pacing by using NCB-PU-based bioelectronics. Evolution of ECG potentials for a rate model, commencing from a normal physiological state, transitioning through a simulated atrioventricular block, followed by the application of electrical stimulation, and culminating with the withdrawal of such stimulation.

integration of the electrodes with the skins. Furthermore, the wearable electrodes can be recycled and reprocessed into a 4×4 electrode array (Figure 4f), which also demonstrated an impressive 80% accuracy in the same tactile perception test (Figure 4g).

2.5. NCB-PU-Based Bioelectronics for In Vivo ECG Recording and Cardiac Pacing

The exceptional flexibility and biocompatibility of our NCB-PU vitrimers confer significant advantages for in vivo implantable bioelectronics. Figure 5a illustrates the in vivo epicardial recording and electrical pacing using NCP-PU-based bioelectronics implanted on a rat's heart. The inherent flexibility of the NCP-PU-based bioelectronics ensures conformal contact with the beating heart, enabling long-term and reliable electrical functionality. All five channels of the NCP-PU-based bioelectronics functioned well, with an average heart rate of approximately 380 beats per minute, indicating that the device does not disrupt the heart's natural rhythm (Figure 5b). The seamless integration enables high-fidelity monitoring (signal-to-noise ratio, SNR \approx 45) across all five channels, surpassing commercial metallic electrodes (SNR \approx 10, Figure 5c). It is worth noting that the recycled electrodes maintain high-quality epicardial recording capabilities

(SNR \approx 40) through a solution-assisted recovery process. To further demonstrate the potential of the NCP-PU-based bioelectronics for cardiac pacing, intermittent electrical pulses (0.4 ms, 0.8 V) were administered to achieve ventricular capture. To create an AV block model, adenosine (AD) was administered intravenously through the tail vein to decrease the heart rate (see Experimental Section for details). As depicted in Figure 5d, epicardial ECG measurements showed distinct pacing spikes at a higher frequency (\approx 480 bpm) and an amplified QRS complex, in contrast to the sinus rhythm observed in the absence of electrical stimulation (\approx 380 bpm). This result confirmed that the electrode's efficacy in modulating the heart's rate and rhythm, functioning akin to a cardiac pacemaker. The cessation of electrical stimulation resulted in the reversion of the heart rate and rhythm to their normal physiological conditions. These results indicate that the NCP-PU vitrimers are a promising flexible substrate material, suitable as a soft coupling interface for a variety of implantable bioelectronics applications.

3. Conclusion

In summary, we have reported a class of recyclable PU vitrimers based on dynamic boronic ester bonds, which function as soft substrates and encapsulants for a range of bioelectronics

applications. The elastomeric nature of these PU vitrimers enables them to form mechanically-compliant interfaces with biological tissues, facilitating high-quality electrophysiological recording and stimulation. Moreover, this unique dynamic cross-linked network allows for the recyclability of PU vitrimers in both solid and liquid phases, thereby facilitating the recycling and reprocessing of bioelectronics. The integration of boronic ester bonds into various polymer architectures offers a promising pathway for developing recyclable flexible substrates and encapsulants in the field of bioelectronics, with the potential to significantly reduce electronic waste and mitigate the associated environmental impact.

4. Experimental Section

Synthesis of NCB-PU Vitrimers: PEG (1.14 g, 1.9 mmol) and IPDI (0.84 g, 3.8 mmol) were fed within a reactor under N_2 atmosphere. DBTDL catalyst (6 μL) was then added and the mixture was kept stirring at 65 °C for 2.5 h to yield prepolymer 1. Subsequently, 5 mL of anhydrous DMF was added to dissolve the prepolymer 1 and the mixture was stirred at 65 °C for another 2 h. NCBC (0.4 g, 1.43 mmol) in 5 mL of dry DMF and IPDI in 2 mL of dry DMF were added to the prepolymer 1 solution in turn. After reacting at 65 °C for 3 h, TMP (0.13 g, 0.95 mmol) in 5 mL of dry DMF was added, and the reaction was further continued at 65 °C for 3 h. Finally, the viscous solution was poured into a PTFE plate, and heated at 90 °C for 18 h under vacuum until the reaction was completed.

Reprocessing of NCB-PU Vitrimer: For the solid phase recycling of NCB-PU vitrimers, the samples were cut into small pieces and placed within a metallic mold. It was then subjected to a hot press at 130 °C and 2 MPa for 15 min to reconstitute the bulk material. Subsequently, the reprocessed samples were cooled down to room temperature for further measurements.

Recycling of NCB-PU Vitrimer by Solvent Treatment: For the liquid phase recycling of NCB-PU vitrimer, an 846.5 mg sample was placed within a 25-mL vial, loaded with 12-mL DMF. The vial was then supplemented with 3-mL H_2O and heated to 130 °C. Within a period of 2 h, the sample degraded completely. The resulting solution was transferred into a PTFE mold and subjected to heating at 100 °C. Following a 2-h treatment, the solvent was completely evaporated, enabling the reconstitution of NCB-PU vitrimers.

Fabrication of the NCB-PU-based Wearable Electrodes: A NCB-PU film with a size of 10 × 10 cm (thickness ≈ 200 μm) was prepared and utilized as a flexible substrate for wearable electronics. A 3D printer (Regenovo) was employed to print conductive silver ink onto the NCB-PU substrate, followed by air drying to form a conductive electrode array. The printing pathways were designed by utilizing the commercially available software Solidworks (Dassault Systemes), before being converted into G-code to direct the 3D (x, y, z) motion control of the printer's nozzles.

Experiments with Human Subjects: Experiments involving human subjects were carried out in accordance with ethical guidelines and approved by the Southern University of Science and Technology (Protocol Number: 2024PES303). Five volunteers participated in this experiment, and the people's image depicted in Figure 4 is Liangjie Shan, who has granted permission for the publication of his images. All volunteers were instructed by professional experimenters on how to use the wearable electronics until they were familiar with the sensation of electrical stimulation. Prior to the experiments, volunteers were directed to clean their hands using alcohol and subsequently apply a thin coat of conductive hydrogel. Each volunteer completed a 20-minute familiarization phase to adapt to the task before beginning any recognition tests. Throughout the electrical stimulation phase, a 20-kHz square wave frequency was employed as the consistent carrier wave across all experimental trials, with the stimulation voltage adjusted according to the volunteer's perceived condition.

Experiments on Animal Subjects: All animal procedures were conducted in accordance with protocols approved by the Committee on Ani-

mal Care at the Southern University of Science and Technology (Protocol Number: SUSTech-JY202308104). Sprague-Dawley rats were anesthetized unconscious with tribromoethanol and securely fastened in a mechanical restraint system prior to tracheal intubation. Subsequently, they were connected to a mechanical ventilator (RWD model R415). After achieving general anesthesia, a thoracic incision was made between the third and fourth left intercostal spaces to expose the heart for surgical access. The pericardium was carefully dissected using fine forceps, and gauze was used to absorb excess biofluids. With the heart's anterior surface exposed, a 5-channel NCP-PU-based bioelectronic device was gently applied to the ventricular surface for ECG recording, and a 0.5 mm diameter metal wire was placed subcutaneously in the leg as a reference electrode. To elicit an atrioventricular block, 200 μL of adenosine at a concentration of 5 mg mL^{-1} was infused intravenously, succeeded by the application of electrical stimulation. The electrical stimulation parameters were set at 0.8 V, with a pulse duration of 4 ms and a frequency of 8 Hz. Additionally, ECG recordings were obtained using commercial electrodes as a control for comparative analysis.

Statistical Analysis: All results are presented as the mean ± standard deviation (SD). All experiments were repeated at least three times and each condition was analyzed in triplicate. Data distribution was assumed to be normal for all parametric tests, but not formally tested, and no significant difference analysis was performed. All statistical analyses were carried out with the Origin software package.

Supporting Information

Supporting Information is available from the Wiley Online Library or from the author.

Acknowledgements

Y.T. and Y.X. contributed equally to this work. J.L. acknowledged the financial support from STI 2030-Major Projects (2022ZZD0209500), National Natural Science Foundation of China (52373139), Natural Science Foundation of Guangdong Province (2022A1515010152 and 2021A1515110735), Basic Research Program of Shenzhen (20231116101626002), the Key Talent Recruitment Program of Guangdong Province (2019QN01Y576). This work was also supported in part by the Science, Technology, and Innovation Commission of Shenzhen Municipality (ZDSYS20220527171403009). The authors also would also like to acknowledge the technical support from SUSTech Core Research Facilities. The authors would like to thank Prof. Shujuan Wang at Xi'an Jiaotong University for her help with the synthesis details on NCB compounds.

Conflict of Interest

The authors declare no conflict of interest.

Data Availability Statement

The data that support the findings of this study are available from the corresponding author upon reasonable request.

Keywords

biointerface, boron–nitrogen coordination, recyclable, sustainable bioelectronics, vitrimers

Received: September 19, 2024

Revised: October 5, 2024

Published online: October 17, 2024

- [1] C. Zhao, J. Park, S. E. Root, Z. Bao, *Nat. Rev. Bioeng.* **2024**, *2*, 671.
- [2] J. Kim, A. S. Campbell, B. E.-F. de Ávila, J. Wang, *Nat. Biotechnol.* **2019**, *37*, 389.
- [3] H. Yuk, B. Lu, X. Zhao, *Chem. Soc. Rev.* **2019**, *48*, 1642.
- [4] M. Lin, H. Hu, S. Zhou, S. Xu, *Nat. Rev. Mater.* **2022**, *7*, 850.
- [5] J. Kang, J. B. H. Tok, Z. Bao, *Nat. Electron.* **2019**, *2*, 144.
- [6] D. A. Weitz, *Nat. Mater.* **2022**, *21*, 986.
- [7] S. Gong, Y. Lu, J. Yin, A. Levin, W. Cheng, *Chem. Rev.* **2024**, *124*, 455.
- [8] S. Kim, S. Baek, R. Sluyter, K. Konstantinov, J. H. Kim, S. Kim, Y. H. Kim, *EcoMat* **2023**, *5*, 12356.
- [9] M. Heacock, C. B. Kelly, K. A. Asante, L. S. Birnbaum, Å. L. Bergman, M.-N. Bruné, I. Buka, D. O. Carpenter, A. Chen, X. Huo, M. Kamel, P. J. Landrigan, F. Magalini, F. Diaz-Barriga, M. Neira, M. Omar, A. Pascale, M. Ruchirawat, L. Sly, P. D. Sly, M. Van den Berg, W. A. Suk, *Environ. Health Persp.* **2016**, *124*, 550.
- [10] R. Rautela, S. Arya, S. Vishwakarma, J. Lee, K. H. Kim, S. Kumar, *Sci. Total Environ.* **2021**, *773*, 145623.
- [11] X. Wang, Y. Gu, Z. Xiong, Z. Cui, T. Zhang, *Adv. Mater.* **2013**, *26*, 1336.
- [12] Y. Xue, J. Zhang, X. Chen, J. Zhang, G. Chen, K. Zhang, J. Lin, C. Guo, J. Liu, *Adv. Funct. Mater.* **2021**, *31*, 2106446.
- [13] Y. Guo, S. Chen, L. Sun, L. Yang, L. Zhang, J. Lou, Z. You, *Adv. Funct. Mater.* **2021**, *31*, 2009799.
- [14] M. S. Brown, L. Somma, M. Mendoza, Y. Noh, G. J. Mahler, A. Koh, *Nat. Commun.* **2022**, *13*, 3727.
- [15] H. R. Lim, H. S. Kim, R. Qazi, Y. T. Kwon, J. W. Jeong, W. H. Yeo, *Adv. Mater.* **2019**, *32*, 201901924.
- [16] Y. Guo, L. Yang, L. Zhang, S. Chen, L. Sun, S. Gu, Z. You, *Adv. Funct. Mater.* **2021**, *31*, 2106281.
- [17] S. Kim, J. Kang, I. Lee, J. Jang, C. B. Park, W. Lee, B.-S. Bae, *npj Flex. Electron.* **2023**, *7*, 33.
- [18] D. Qi, K. Zhang, G. Tian, B. Jiang, Y. Huang, *Adv. Mater.* **2020**, *33*, 2003155.
- [19] K. Liu, Y. Jiang, Z. Bao, X. Yan, *CCS Chem.* **2019**, *1*, 431.
- [20] J. Kang, D. Son, G. N. Wang, Y. Liu, J. Lopez, Y. Kim, J. Y. Oh, T. Katsumata, J. Mun, Y. Lee, L. Jin, J. B. Tok, Z. Bao, *Adv. Mater.* **2018**, *30*, 1706846.
- [21] J. Y. Oh, S. Rondeau-Gagné, Y. C. Chiu, A. Chortos, F. Lissel, G. J. N. Wang, B. C. Schroeder, T. Kurosawa, J. Lopez, T. Katsumata, J. Xu, C. Zhu, X. Gu, W. G. Bae, Y. Kim, L. Jin, J. W. Chung, J. B. H. Tok, Z. Bao, *Nature* **2016**, *539*, 411.
- [22] J. Hou, M. Liu, H. Zhang, Y. Song, X. Jiang, A. Yu, L. Jiang, B. Su, *J. Mater. Chem. A.* **2017**, *5*, 13138.
- [23] C. J. Kloxin, T. F. Scott, B. J. Adzima, C. N. Bowman, *Macromolecules* **2010**, *43*, 2643.
- [24] C. N. Bowman, C. J. Kloxin, *Angew. Chem., Int. Ed.* **2012**, *51*, 4272.
- [25] C. J. Kloxin, C. N. Bowman, *Chem. Soc. Rev.* **2013**, *42*, 7161.
- [26] Z. P. Zhang, M. Z. Rong, M. Q. Zhang, *Prog. Polym. Sci.* **2018**, *80*, 39.
- [27] Y. Jin, C. Yu, R. J. Denman, W. Zhang, *Chem. Soc. Rev.* **2013**, *42*, 6634.
- [28] G. M. Scheutz, J. J. Lessard, M. B. Sims, B. S. Sumerlin, *J. Am. Chem. Soc.* **2019**, *141*, 16181.
- [29] W. Zou, J. Dong, Y. Luo, Q. Zhao, T. Xie, *Adv. Mater.* **2017**, *29*, 1606100.
- [30] D. Montarnal, M. Capelot, F. Tournilhac, L. Leibler, *Science* **2011**, *334*, 965.
- [31] J. Zheng, Z. M. Png, S. H. Ng, G. X. Tham, E. Ye, S. S. Goh, X. J. Loh, Z. Li, *Mater. Today* **2021**, *51*, 586.
- [32] Y. Tao, X. Liang, J. Zhang, I. M. Lei, J. Liu, *J. Polym. Sci.* **2023**, *61*, 2233.
- [33] N. J. Van Zee, R. Nicolay, *Prog. Polym. Sci.* **2020**, *104*, 101233.
- [34] W. Denissen, J. M. Winne, F. E. Du Prez, *Chem. Sci.* **2016**, *7*, 30.
- [35] O. R. Cromwell, J. Chung, Z. Guan, *J. Am. Chem. Soc.* **2015**, *137*, 6492.
- [36] H. Ying, Y. Zhang, J. Cheng, *Nat. Commun.* **2014**, *5*, 3218.
- [37] W. L. Brooks, B. S. Sumerlin, *Chem. Rev.* **2016**, *116*, 1375.
- [38] J. P. Brutman, P. A. Delgado, M. A. Hillmyer, *ACS Macro Lett.* **2014**, *3*, 607.
- [39] D. T. Sheppard, K. Jin, L. S. Hamachi, W. Dean, D. J. Fortman, C. J. Ellison, W. R. Dichtel, *ACS Cent. Sci.* **2020**, *6*, 921.
- [40] J. A. Chiong, Y. Zheng, S. Zhang, G. Ma, Y. Wu, G. Ngaruka, Y. Lin, X. Gu, Z. Bao, *J. Am. Chem. Soc.* **2022**, *144*, 3717.
- [41] P. Taynton, H. Ni, C. Zhu, K. Yu, S. Loob, Y. Jin, H. J. Qi, W. Zhang, *Adv. Mater.* **2016**, *28*, 2904.
- [42] X. Zhang, S. Wang, Z. Jiang, Y. Li, X. Jing, *J. Am. Chem. Soc.* **2020**, *142*, 21852.
- [43] Y. Guo, S. Chen, L. Sun, L. Yang, L. Zhang, J. Lou, Z. You, *Adv. Funct. Mater.* **2020**, *31*, 2009799.
- [44] Z. Lei, H. Chen, Y. Jin, W. Zhang, *Cell Rep. Phys. Sci.* **2023**, *4*, 101336.
- [45] Z. Zou, C. Zhu, Y. Li, X. Lei, W. Zhang, J. Xiao, *Sci. Adv.* **2018**, *4*, eaaoq0508.
- [46] C. Shi, Z. Zou, Z. Lei, P. Zhu, W. Zhang, J. Xiao, *Sci. Adv.* **2020**, *6*, eabd0202.
- [47] C. Shi, Z. Zou, Z. Lei, P. Zhu, G. Nie, W. Zhang, J. Xiao, *Research* **2021**, *2021*, 9846036.
- [48] H.-W. Engels, H.-G. Pirk, R. Albers, R. W. Albach, J. Krause, A. Hoffmann, H. Casselmann, J. Dormish, *Angew. Chem., Int. Ed.* **2013**, *52*, 9422.
- [49] M. Röttger, T. Domenech, R. van der Weegen, A. Breuillac, R. Nicolay, L. Leibler, *Science* **2017**, *356*, 62.
- [50] Z. H. Zhao, P. C. Zhao, Y. Zhao, J. L. Zuo, C. H. Li, *Adv. Funct. Mater.* **2022**, *32*, 2201959.
- [51] Z. H. Zhao, P. C. Zhao, S. Y. Chen, Y. X. Zheng, J. L. Zuo, C. H. Li, *Angew. Chem., Int. Ed.* **2023**, *135*, 202301993.
- [52] Y. Shi, Y. Zeng, P. Kucheryavy, X. Yin, K. Zhang, G. Meng, J. Chen, Q. Zhu, N. Wang, X. Zheng, F. Jäkle, P. Chen, *Angew. Chem., Int. Ed.* **2022**, *61*, 202213615.
- [53] J. Liu, C. S. Y. Tan, Z. Yu, Y. Lan, C. Abell, O. A. Scherman, *Adv. Mater.* **2017**, *29*, 1604951.
- [54] J. Liu, C. S. Y. Tan, Z. Yu, N. Li, C. Abell, O. A. Scherman, *Adv. Mater.* **2017**, *29*, 1605325.
- [55] M. Gosecki, M. Gosecka, *Polymers* **2022**, *14*, 842.
- [56] X. Zhang, Y. Zhao, S. Wang, X. Jing, *Mater. Chem. Front.* **2021**, *5*, 5534.
- [57] Z. Zhang, A. K. Biswal, A. Nandi, K. Frost, J. A. Smith, B. H. Nguyen, S. Patel, A. Vashisth, V. Iyer, *Nat. Sustain.* **2024**, *7*, 616.
- [58] M. Moroni, M. R. Servin-Vences, R. Fleischer, O. Sánchez-Carranza, G. R. Lewin, *Nat. Commun.* **2018**, *9*, 1096.
- [59] W. Lin, D. Zhang, W. W. Lee, X. Li, Y. Hong, Q. Pan, R. Zhang, G. Peng, H. Z. Tan, Z. Zhang, L. Wei, Z. Yang, *Sci. Adv.* **2022**, *8*, eabp8738.
- [60] P. Zhang, I. M. Lei, G. Chen, J. Lin, X. Chen, J. Zhang, C. Cai, X. Liang, J. Liu, *Nat. Commun.* **2022**, *13*, 4775.
- [61] F. Wang, Y. Xue, X. Chen, P. Zhang, L. Shan, Q. Duan, J. Xing, Y. Lan, B. Lu, J. Liu, *Adv. Funct. Mater.* **2024**, *34*, 2314471.